Available online at www.sciencedirect.com

ScienceDirect

Catalysis Today 131 (2008) 179–187

CATALYSIS TODAY

www.elsevier.com/locate/cattod

Effect of Rh loading on the performance of Rh/Al_2O_3 for methane partial oxidation to synthesis gas

Jian-Mei Li, Fei-Yang Huang, Wei-Zheng Weng *, Xiao-Qing Pei,
Chun-Rong Luo, Hai-Qiang Lin, Chuan-Jing Huang, Hui-Lin Wan *

State Key Laboratory of Physical Chemistry of Solid Surfaces and Department of Chemistry,
College of Chemistry and Chemical Engineering, Xiamen University, Xiamen 361005, China

Abstract

Catalytic performance for partial oxidation of methane (POM) to synthesis gas was studied over the Rh/Al_2O_3 catalysts with Rh loadings between 0.1 and 3 wt%. It was found that the ignition temperature of POM reaction increased with the decreasing of the Rh loadings in the catalysts. For the POM reaction over the catalysts with high ($\geq$1 wt%) Rh loadings, steady-state reactivity was observed. For the reaction over the catalysts with low ($\leq$0.25 wt%) Rh loadings, however, oscillations in CH_4 and reaction products (CO, H_2, and CO_2) were observed. Comparative studies using H_2-TPR, O_2-TPD and high temperature *in situ* Raman spectroscopy techniques were carried out in order to elucidate the relation between the redox property of the Rh species in the Rh/Al_2O_3 with different Rh loadings and the performance of the catalysts for the reaction. Three kinds of oxidized rhodium species, i.e. the rhodium oxide species insignificantly affected by the support (RhO_x), that intimately interacting with the Al_2O_3 surface (Rh^iO_x) and the $Rh(AlO_2)_y$ species formed by diffusion of rhodium oxides in to sublayers of Al_2O_3 [C.P. Hwang, C.T. Yeh, Q.M. Zhu, Catal. Today, 51 (1999) 93.], were identified by H_2-TPR and O_2-TPD experiments. Among them, the first two species can be easily reduced by H_2 at temperature below 350 °C, while the last one can only be reduced by H_2 at temperature above 500 °C. The ignition temperatures of POM reaction over the catalysts are closely related to the temperature at which most of the RhO_x and Rh^iO_x species can be reduced by CH_4 in the reaction mixture. Compared to the Rh/Al_2O_3 with high Rh loadings, the catalysts with low Rh loadings contain more Rh^iO_x species which possess stronger Rh–O bond strength and are more difficult to be reduced than RhO_x by the reaction mixture. Higher temperature is therefore required to ignite the POM reaction over the catalysts with lower Rh loadings. The oscillation during the POM reaction over the Rh/Al_2O_3 with low Rh loadings can be related to the behaviour of $Rh(AlO_2)_y$ species in the catalyst switching cyclically from the oxidized state to the reduced state during the reaction.

Keywords: Methane partial oxidation; Synthesis gas; Rh/Al_2O_3; Rh loading; Oscillation; *In situ* Raman

1. Introduction

The partial oxidation of methane (POM) to produce CO and H_2 has received increasing attention in recent years, mainly because of its potential application as a commercial source of synthesis gas [1–4]. The elucidation of reaction pathways in POM to synthesis gas over supported transition metal catalysts is an important pre-requisite toward improved catalyst designs. It is also one of the basic step and the major challenge in the study of the reaction [5]. Although numerous attempts have been made to understand the reaction mechanism, there is a still ongoing discussion whether synthesis gas is form via direct partial oxidation route [3] or via the reforming reactions after combustion of CH_4 [1]. It was found that the reaction mechanism might depend on the chemical state of the catalyst surface as well as on the type and amount of oxygen species available [6–17]. It was also reported that catalyst supports might play a significant role in affecting activity, selectivity and stability of catalysts as well as the reaction mechanism [11,13,18–32].

Al_2O_3 supported Rh catalyst exhibits high stability with excellent activity and selectivity for the reaction and has been extensively studied [11,13,14,32–37]. From the economical point of view, a catalyst of low Rh loading with high metal dispersion is preferred in order to achieve a high accessibility of

---

* Corresponding authors. Fax: +86 592 2183047.
E-mail addresses: wzweng@xmu.edu.cn (W.-Z. Weng), hlwan@xmu.edu.cn (H.-L. Wan).

0920-5861/$ – see front matter © 2007 Elsevier B.V. All rights reserved.
doi:10.1016/j.cattod.2007.10.040

catalytically active noble metal. On the other hand, due to the interaction between Rh and Al_2O_3, the Rh species in the catalysts with low metal loadings will be more significantly affected by Al_2O_3 than those on the samples with high metal loadings. It is found that Al_2O_3 is not inert concerning the adsorption and storage of oxygen [11] and may have a significant influence on the activity of Rh catalyst [32]. The participation of OH groups on the γ-Al_2O_3 during the POM reaction has been shown by Hofstad et al. [11] and Wang et al. [13]. Even the mechanisms of POM to synthesis gas over Rh/γ-Al_2O_3 were found to depend on the Rh loading [37]. At low metal loadings, the combustion-reforming mechanism is responsible for the reaction, while at high loadings a combination of the combustion-reforming and pyrolysis-oxidation mechanisms is responsible at low temperatures ($\leq$500 °C) and the pyrolysis-oxidation mechanism becomes dominant at high temperatures ($\geq$650 °C).

The aim of the present study is to investigate the nature of the Rh species in the Rh/Al_2O_3 with Rh loadings from 0.1 to 3 wt% using H_2-temperature-programmed reduction (H_2-TPR), O_2-temperature-programmed desorption (O_2-TPD) and high temperature *in situ* Raman spectroscopy techniques. The results of above characterizations are related to the catalytic performance of the catalysts at the temperature ranging from 300 to 600 °C. It is expected that the experiments should provide with some useful information to understand the effects of metal-support interaction on the nature of the rhodium species over Al_2O_3 and its relationship with the catalytic performance of the catalysts for methane partial oxidation to synthesis gas.

2. Experimental

2.1. Catalyst preparations

Rh/Al_2O_3 and Rh/SiO_2 catalysts were prepared by the wet impregnation method using $RhCl_3 \cdot nH_2O$ (38 wt% Rh) as the precursor for the metal. Most of the Rh/Al_2O_3 catalysts used in the study were prepared using the Al_2O_3 from Guizhou Alumina Factory, China (TL-02, ~250 m^2/g). The Rh/Al_2O_3 catalysts used in the O_2-TPD experiments were prepared using the Al_2O_3 from China Medicine (Group) Shanghai Chemical Reagent Corporation (~210 m^2/g). The Rh/SiO_2 catalyst was prepared using the SiO_2 from Aldrich (60 A, ~480 m^2/g). The Al_2O_3 and SiO_2 supports were calcined at 300 °C for 1 h before using. After noble metal impregnation, the catalyst was dried at 110 °C and calcined at 600 °C in the air for 4 h. The fresh catalysts were then reduced with H_2 at 600 °C for 30 min before subjecting to tests.

2.2. The performance of catalysts

The catalytic performance of the catalysts for POM to synthesis gas was studied using $CH_4/O_2/Ar = 2/1/45$ mixture (in the volume ratio) as a reaction feed. The reaction was carried out in a fixed-bed quartz tube reactor (5 mm i. d.) at the atmospheric pressure. The catalyst (15.0 mg) was reduced at 600 °C for 30 min before it was switched to take the reaction feed. The products were analyzed by an on-line GC equipped with a thermal conductivity detector (TCD) using Ar (99.999%, Linde) as the carrier gas and a carbon sieve column (1.5 m) for the separation of CH_4, O_2, H_2, CO and CO_2. In some experiments, a quadrupole mass spectrometer (Pfeiffer, model ThermoStar GSD301T2) was employed to analyze the composition of the reaction products. Ions at 2 (H_2), 15 (CH_4), 18 (H_2O), 28 (CO), 32 (O_2) and 44 (CO_2) *m/e* values were detected during on-line measurements.

2.3. Catalyst characterization

X-ray powder diffraction (XRD) analysis was carried out by a Panalytical X'pert PRO diffractometer scanning 2θ from 10 to 80°. Cu Kα radiation operated at 40 kV and 30 mA was used as the X-ray source. The XRD patterns of the Rh/Al_2O_3 catalysts show only the diffraction peaks of γ-Al_2O_3 [38]. No diffraction peak referring to the rhodium oxide or metallic Rh species was detected in the fresh or reduced samples.

The BET (Brunauer-Emmett-Teller) surface area of the catalyst was measured by N_2 adsorption at −196 °C using a Micromeretics Tristar 3000 instrument. Before the measurement, the samples were degassed at 300 °C for 2 h. The results are listed in Table 1. The metal dispersion data of the catalyst was determined by O_2 and H_2 chemisorption at 35 °C assuming the stoichiometry values of O/Rh and H/Rh = 1. The

Table 1
BET surface area and metal dispersion data of the catalysts

Catalyst	BET (m^2/g)	$Rh_{red(600)}/Rh_{total}$[a] × 100%	$O/Rh_{red(600)}$	$H/Rh_{red(600)}$
0.1 wt% Rh/Al_2O_3	181	22.1	2.37	0.48
0.25 wt% Rh/Al_2O_3	183	31.5	1.90	0.49
0.5 wt% Rh/Al_2O_3	182	40.2	1.51	0.74
1 wt% Rh/Al_2O_3	184	58.6	1.06	0.76
1.5 wt% Rh/Al_2O_3	176	64.4	0.94	0.82
2 wt% Rh/Al_2O_3	179	68.8	0.88	0.80
3 wt% Rh/Al_2O_3	185	84.7	0.67	0.75
1 wt% Rh/SiO_2	484	~100	0.28	0.40

[a] $Rh_{red(600)}/Rh_{total}$: Ratio of the Rh species in the catalysts reducible by H_2 at temperature below 600 °C. The data were calculated based on the H_2-TPR profiles shown in Fig. 3.

experiments were performed by a Micromeretics ASAP 2010 instrument. The catalyst sample (0.3–0.6 g) was first reduced with H_2 (99.999%, Linde) at 600 °C for 30 min followed by evacuation at 450 °C for 30 min. The sample was then cooled down to 35 °C under vacuum for analysis. The O/Rh and H/Rh data, after being calibrated with the ratio of the Rh species in the sample reducible by H_2 at 600 °C ($Rh_{red(600)}/Rh_{total}$, determined by H_2-TPR experiment), are listed in Table 1.

The H_2-TPR experiments were performed by a GC-TPR set-up. Prior to the TPR experiment, the catalyst (0.1–0.15 g) was oxidized with $O_2/Ar = 5/95$ mixture (in the volume ratio, 20 mL/min) at 600 °C for 30 min and cooled down to 5 °C under same atmosphere. The sample was then purged with $H_2/Ar = 5/95$ mixture at 5 °C for about 10 min until the base line of the instrument was flat. The TPR profile of the catalyst was obtained by heating the above treated sample from 5 to 800 °C at a rate of 10 °C/min in a flow of $H_2/Ar = 5/95$ mixture (50 mL/min). The hydrogen consumption was monitored by a TCD detector. The O_2-TPD experiments were performed by a Micromeritics AutoChem II 2920 instrument. The catalyst (~0.2 g) was first oxidized with $O_2/He = 1/4$ mixture (in the volume ratio, 20 mL/min) at 500 °C for 30 min and cooled down to 20 °C under same atmosphere. The sample was then purged with He (99.999%, Linde) at 20 °C for 30 min and heated from 20 to 1100 °C at a rate of 10 °C/min in a flow of He (50 mL/min). The O_2 desorption was analyzed by an on-line quadrupole mass spectrometer (Pfeiffer, model ThermoStar GSD301T2).

In situ Raman experiments were performed with a Renishaw R1000 microprobe Raman system equipped with CCD detectors using a home built high temperature *in situ* Raman cell described in a previous paper [39]. The samples were placed in the sample holder equipped with a thermocouple placed underneath for temperature measurement. The excitation wavelengths were 325 nm (He-Cd laser) with a power of ~3 mW and 514.5 nm (Ar^+ laser) with power of ~5 mW measured at the analysis spot. The microscope attachment for the spectrometer is based on a Leica DMLM system using an OFR LMU-15×-NUV (for 325 nm He-Cd laser) and a Leica PL Fluotar 50× (for 514.5 nm Ar^+ laser) objectives.

3. Results and discussion

3.1. Catalytic performance tests

3.1.1. Performance of the catalysts at different temperatures

Table 2 shows the catalytic performance of Rh/Al_2O_3 (0.1–3 wt%) and Rh/SiO_2 (1 wt%) catalysts measured at temperatures indicated in the table during stepwise heating of a previously reduced catalyst under $CH_4/O_2/Ar = 2/1/45$ flow from 30 to 600 °C. It can be seen that the oxidation of CH_4 on Rh/Al_2O_3 starts at the temperatures between 300 and 400 °C, depending on the amount of Rh loading. No CO and H_2 were detected before the complete consumption of O_2. The POM reaction, which can be experimentally determined by the suddenly rapid increase in CH_4 and O_2 conversions, was found to ignite at the temperatures between 440 and 540 °C, and the ignition temperatures for POM reaction were found to decrease with the increasing of Rh loading in the catalysts. Similar results were reported by Wang et al. [37]. It was also found that, although the reactant (at $CH_4/O_2 = 2$) had been diluted with large amount of Ar, the observed CH_4 conversions and CO selectivities on the catalysts were still higher than the thermodynamic equilibrium values at the furnace temperatures [40], indicating that a hot spot layer still exists in the catalyst bed.

Compared to Rh/Al_2O_3 catalysts, the POM reaction on Rh/SiO_2 with comparable amount of Rh loading can be ignited at much lower temperature. These results suggested that both the support material and the Rh loading had a significant impact on the performance of catalyst. The stronger interaction between Rh and Al_2O_3 as compared to that between Rh and SiO_2 should be responsible for higher ignition temperature of POM reaction over Rh/Al_2O_3 catalysts [41,42]. To further elucidate the effect of metal-support interaction on the performance of Rh/Al_2O_3 catalysts for POM reaction, the continuous flow reaction tests over the catalysts with Rh loadings between 0.1 and 1 wt% are performed.

3.1.2. Continuous flow reaction tests

Fig. 1 shows the POM performances of the Rh/Al_2O_3 catalysts with Rh loadings of 0.1, 0.25, 0.5 and 1 wt% at 600 °C (furnace temperature) and at a space velocity (SV) of 2.0×10^5 mL g cat^{-1} h^{-1}. As shown in Fig. 1, steady-state reactivity was observed on 1 wt% Rh/Al_2O_3 catalyst within about 6.5 h on stream. On 0.5 wt% Rh/Al_2O_3, both the conversion of methane and the selectivities of CO and H_2 decreased with the increasing of time on stream. For the reaction over the catalysts with Rh loading of 0.25 wt% or lower, however, oscillations in CH_4 and products (CO, H_2 and CO_2) were observed.

Fig. 2 shows the oscillation cycles followed by a quadrupole mass spectrometer for the reaction over 0.1 wt% Rh/Al_2O_3 at 600 °C (furnace temperature). The signals of the reactants and the products have been vertically offset by the factors shown to the right of each plot to avoid overlapping. It can be seen that the period and amplitude of oscillations are irregular. Large amplitude oscillations proceeded along with the small oscillations. But the waveform of each oscillation cycle is very similar. Oscillations in the signals of CH_4 (one of the reactant) and complete oxidation products (CO_2 and H_2O) are observed to be in-phase with each other, whilst being out-of-phase with the signals of POM reaction products (CO and H_2). The maximum CH_4 conversion is always seen to coincide with the lowest concentrations of CO_2 and H_2O, and highest yields of CO and H_2. The temperature measured by a thermocouple placed at top of the catalyst bed (top line in figure) is also seen to rise and fall with the activity of the catalyst. In general, the temperature oscillation during the reaction is in-phase with the oscillations of CO and H_2. However, compared to other signals shown in Fig. 2, the response of temperature is a little sluggish probably due to the heat capacity of thermocouple. Since most of the O_2 in the reaction mixture was consumed during the reaction, no oscillation in O_2 was observed.

Table 2
Catalytic performance of the catalysts at different temperature

Catalysts	Furnace temperature (°C)	Conv.(%)		Sel.(%)			H_2/CO
		CH_4	O_2	CO	H_2	CO_2	
0.1 wt% Rh/Al_2O_3	350	0	0	0	0	0	/
	400	0.93	3.8	0	0	100	/
	450	2.4	8.3	0	0	100	/
	500	5.5	23.2	0	0	100	/
	540	12.4	50.2	0	0	100	/
	550	**46.6**	**100**	**63.4**	**57.5**	**36.6**	**1.8**
	600	53.6	100	71.2	62.9	28.8	1.8
0.25 wt% Rh/Al_2O_3	350	0	0	0	0	0	/
	400	1.0	4.8	0	0	100	/
	450	3.5	13.8	0	0	100	/
	500	11.9	48.5	0	0	100	/
	510	18.7	76.4	0	0	100	/
	520	**58.9**	**100**	**63.8**	**80.3**	**36.2**	**2.5**
	550	62.6	100	71.9	83.4	28.1	2.3
	600	64.7	100	74.0	79.9	26.0	2.2
0.5 wt% Rh/Al_2O_3	350	0	0	0	0	0	/
	400	1.0	4.7	0	0	100	/
	450	3.5	14.2	0	0	100	/
	480	9.3	38.3	0	0	100	/
	490	**55.1**	**100**	**55.1**	**75.1**	**44.9**	**2.7**
	500	56.1	100	58.3	77.1	41.7	2.6
	550	68.9	100	74.4	81.4	25.6	2.2
	600	79.2	100	85.2	81.3	14.8	1.9
1 wt% Rh/Al_2O_3	300	0	0	0	0	0	/
	350	0.8	2.0	0	0	100	/
	400	2.0	6.2	0	0	100	/
	460	8.0	33.3	0	0	100	/
	470	**51.9**	**100**	**49.3**	**77.3**	**50.7**	**3.1**
	500	58.9	100	58.4	79.8	41.6	2.7
	550	71.8	100	76.0	82.1	24.0	2.2
	600	82.6	100	87.7	83.4	12.3	1.9
2 wt% Rh/Al_2O_3	300	0	0	0	0	0	/
	350	0.59	2.4	0	0	100	/
	400	2.1	8.9	0	0	100	/
	450	11.2	45.5	0	0	100	/
	460	**52.1**	**100**	**47.4**	**74.1**	**52.6**	**3.1**
	500	61.0	100	62.8	80.9	37.2	2.6
	550	73.4	100	78.9	82.7	21.1	2.1
	600	84.0	100	89.7	83.6	10.3	1.9
3 wt% Rh/Al_2O_3	300	0	0	0	0	0	/
	350	1.0	3.5	0	0	100	/
	400	2.4	11.6	0	0	100	/
	430	9.7	41.0	0	0	100	/
	440	**48.0**	**100**	**39.1**	**74.3**	**60.9**	**3.8**
	450	49.9	100	43.2	76.1	56.8	3.5
	500	61.0	100	62.3	81.8	37.7	2.6
	550	73.3	100	77.5	82.2	22.5	2.1
	600	84.1	100	88.9	82.4	11.1	1.9
1 wt% Rh/SiO_2	300	2.5	8.3	0	0	100	/
	350	11.6	45.9	0	0	100	/
	360	22.2	89.2	0	2.3	100	/
	370	**25.0**	**97.5**	**4.2**	**7.6**	**95.8**	**3.7**
	400	29.2	100	16.7	26.4	83.3	3.2
	450	39.0	100	41.3	53.4	58.7	2.6
	500	53.1	100	59.0	72.1	41.0	2.4
	550	68.0	100	75.5	82.9	24.5	2.2
	600	81.6	100	87.7	84.6	12.3	1.9

Reaction condition: $CH_4/O_2/Ar = 2/1/45$, $m_{cat.} = 15$ mg, SV = 2.0×10^5 mL h^{-1} g^{-1}. Catalysts were reduced with H_2 at 600 °C before testing. Data were collected after 20 min on stream.

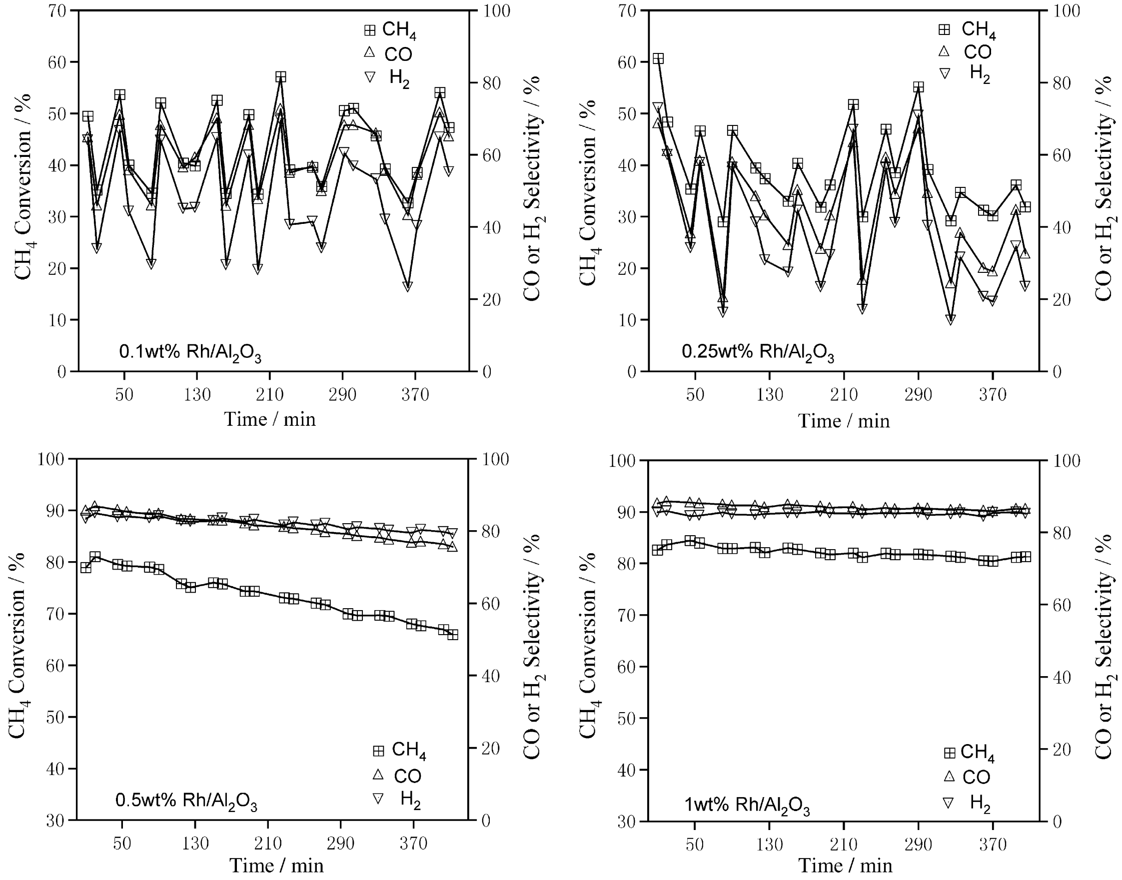

Fig. 1. Catalytic performance of the Rh/Al_2O_3 catalysts with different Rh loadings at 600 °C. Reaction condition: $CH_4/O_2/Ar = 2/1/45$, $m_{cat.} = 15$ mg, $SV = 2.0 \times 10^5$ mL h^{-1} g^{-1}. Catalysts were reduced with H_2 at 600 °C before testing.

As shown in Fig. 2, each oscillation cycle starts with a rapid increase in the signals of CO and H_2. Even for a large oscillation cycle, the maximum concentrations of CO and H_2 can be reached within 2–3 s. The signals of CO and H_2 are then gradually decrease in intensity. For a large oscillation cycle, it will take more than several minutes for the signals of CO and H_2 to be back to the minimum level. The responses of CH_4, CO_2 and H_2O signals during the above period are almost in counter phase with the signals of CO and H_2. The oscillatory behaviour is no longer observed when furnace temperature is raised to 850 °C.

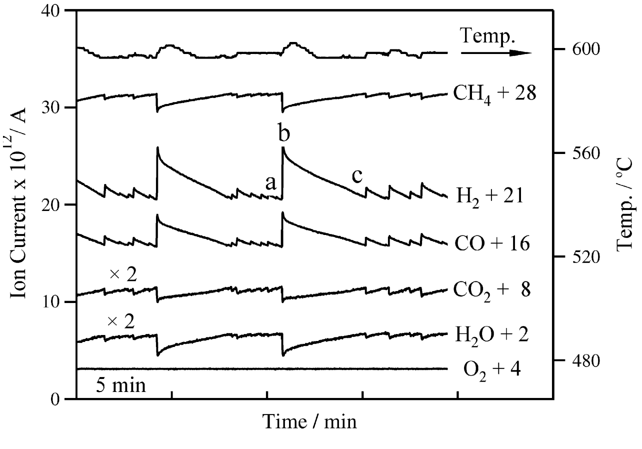

Fig. 2. Oscillations of methane partial oxidation to synthesis gas over 0.1 wt% Rh/Al_2O_3 at 600 °C (furnace temperature). The top line shows the temperature oscillation at the top of the catalyst bed during the reaction. Feed: $CH_4/O_2/Ar = 2/1/45$. Catalysts were reduced with H_2 at 600 °C before testing.

The oscillatory behaviour during methane partial oxidation reaction has also been found on the Ni, Co and Pd wires and foils [43–48], as well as on 0.1 wt% Rh/α-Al_2O_3 [49], Rh/H-ZSM-5 [50] and 1 wt% Rh/γ-Al_2O_3 calcined at 900 °C [39]. According to the literature, the oscillatory behaviour can be related to the periodic oxidation and reduction of the metal species during the reaction [43–48]. These results suggest that the redox property of the rhodium species in the Rh/Al_2O_3 catalysts with Rh loadings ≤ 0.25 wt% are very different from that in the samples with Rh loadings higher than 1 wt%. From the results of O_2 and H_2 chemisorption over the Rh/Al_2O_3 with different Rh loadings (Table 1), it can be seen that the Rh species in the catalysts with Rh loadings ≤ 0.25 wt% show much higher $O/Rh_{red(600)}$ values (1.90–2.37) than those in the samples with Rh loadings higher than 1 wt% (0.67–1.06) in the O_2 chemisorption experiments, indicating that the Rh species in the former samples are more easily oxidized than those in the latter one. Further evidence will be provided by the experiments of H_2-TPR and O_2-TPD shown in the following section.

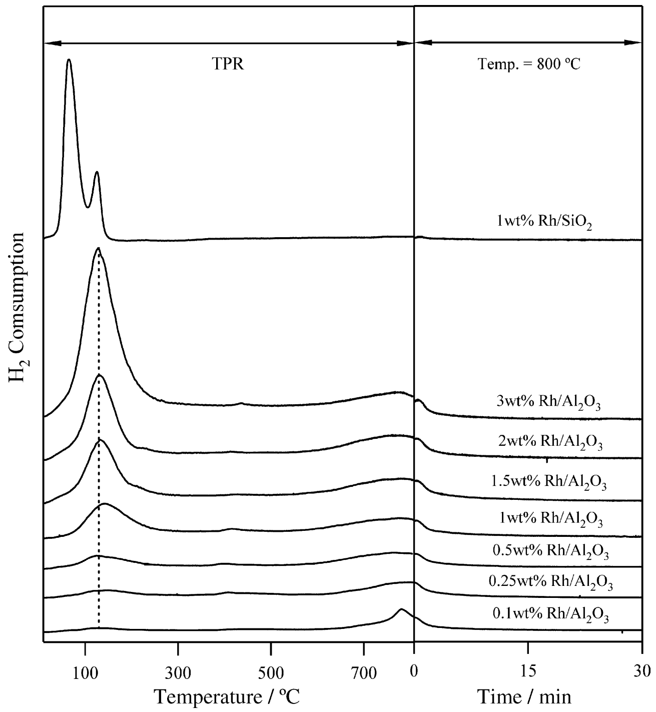

Fig. 3. H_2-TPR profiles of 1 wt% Rh/SiO_2 and the Rh/Al_2O_3 catalysts with different Rh loadings. Before experiments, the fresh catalysts were reduced with H_2/Ar = 5/95 at 600 °C for 30 min followed by reoxidized with O_2/Ar = 5/95 at 600 °C for 30 min.

3.2. H_2-TPR and O_2-TPD characterizations

The H_2-TPR profiles of the catalysts are shown in Fig. 3. The quantified figures of the TPR profiles for the catalysts are shown in Table 3. Each TPR curve of the Rh/Al_2O_3 catalysts are composed of two reduction peaks with temperature maxima (T_m) at ~130 and >750 °C, respectively. According to the results of Hwang et al. [41], the TPR peak with T_m below 350 °C can be attributed to the reduction of two kinds of rhodium oxide species with different extent of interaction with Al_2O_3, i.e. the rhodium oxide species insignificantly affected by the support (RhO_x) and that intimately interacting with the Al_2O_3 surface (Rh^iO_x). The latter is more difficult to be reduced than the former. The broad peak at temperature above 500 °C can be attributed to the reduction of $Rh(AlO_2)_y$ species formed by diffusion of rhodium oxides into sublayers of Al_2O_3 structure as a result of high temperature (>500 °C) oxidation [41]. Due to the metal-support interaction between Rh and Al_2O_3 [41,42], the relative intensities of these TPR peaks varied significantly with the Rh loadings. The amount of $Rh(AlO_2)_y$ species were found to increase significantly with the decreasing of Rh loadings. The position of the low temperature TPR peak (T_m ~130 °C) was also found to shift towards high temperature direction with the decreasing of Rh loadings. The catalysts with Rh loadings below 0.25 wt% consist mainly of $Rh(AlO_2)_y$ species (≥70%) which can only be reduced with H_2 at the temperature above 500 °C. Compared to Rh/Al_2O_3 catalysts, reduction of the rhodium oxide species supported on SiO_2 took place at lower temperature. The TPR peaks with the temperature maxima at 65 and 125 °C were observed on 1 wt% Rh/SiO_2, and no reduction peak was observed in the high temperature region. This observation can be explained by that the metal-support interaction between Rh and SiO_2 is much weaker than that between Rh and Al_2O_3. To further elucidate the nature of the oxidized rhodium species in the Rh/Al_2O_3 catalysts of different Rh loadings, O_2-TPD experiments were carried out.

Fig. 4 shows the O_2-TPD profiles of Rh/Al_2O_3 and Rh/SiO_2 catalysts. Because the interaction between Rh and Al_2O_3 is much stronger than that between Rh and SiO_2, the temperature

Table 3
Quantification of the TPR signals for the catalysts

Catalyst	Reduction temperature (°C)	Percentage (%)
0.1 wt% Rh/Al_2O_3	<350	20.9
	>500	79.1
0.25 wt% Rh/Al_2O_3	<350	29.6
	>500	70.4
0.5 wt% Rh/Al_2O_3	<350	38.2
	>500	61.8
1 wt% Rh/Al_2O_3	<350	56.7
	>500	43.3
1.5 wt% Rh/Al_2O_3	<350	62.7
	>500	37.3
2 wt% Rh/Al_2O_3	<350	67.9
	>500	32.1
3 wt% Rh/Al_2O_3	<350	83.6
	>500	16.4
1 wt% Rh/SiO_2	<250	~100

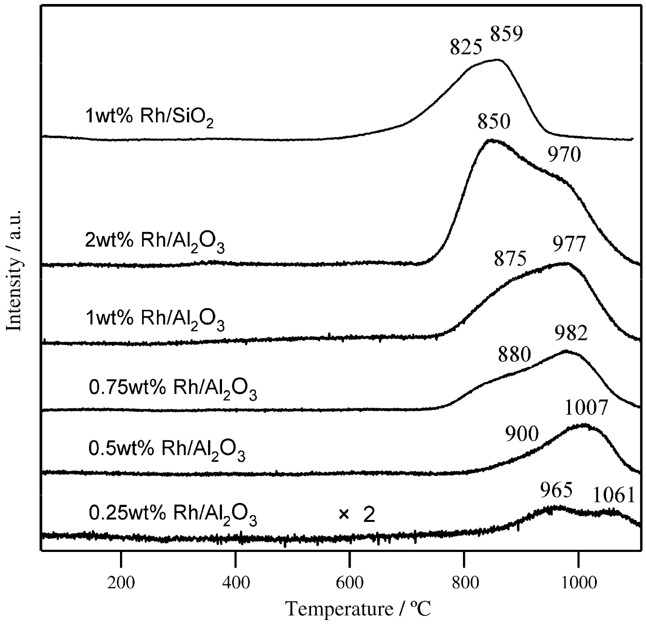

Fig. 4. O_2-TPD profiles of 1 wt% Rh/SiO_2 and the Rh/Al_2O_3 catalysts with different Rh loadings. Before experiments, the fresh catalysts were reduced with H_2/Ar = 5/95 at 600 °C for 30 min followed by reoxidized with O_2/He = 1/4 at 500 °C for 30 min.

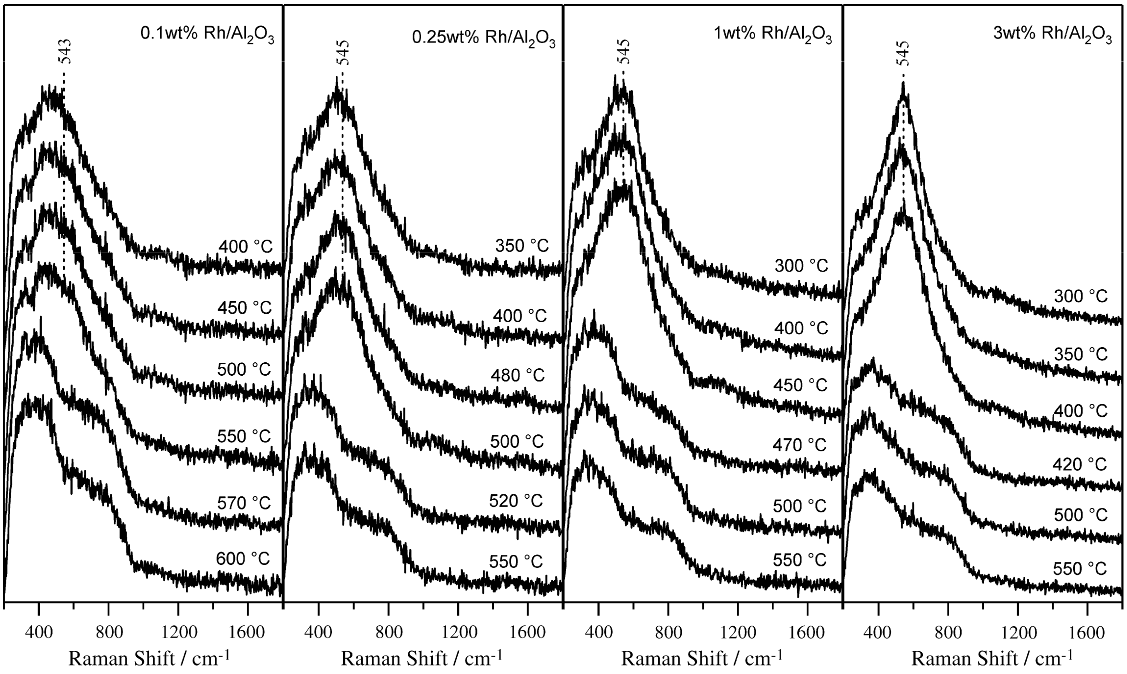

Fig. 5. Raman spectra of the Rh/Al_2O_3 catalysts recorded at the indicated temperature during stepwise heating of the previously reduced samples under $CH_4/O_2/Ar = 2/1/45$ atmosphere from 30 to 600 °C.

maxima of the O_2 desorption peaks on Rh/Al_2O_3 samples are higher than those on Rh/SiO_2, which is also in agreement with the results of H_2-TPR experiments shown above. Each O_2-TPD profile of Rh/Al_2O_3 consists of two O_2 desorption peaks attributable to two kinds of oxidized Rh species in the samples. Based on the results of our previous of O_2-TPD and H_2-TPR studies on the Rh/Al_2O_3 catalyst calcined at 600 and 900 °C [39], the desorption peaks with maxima at 870–880 °C and 970–980 °C can be attributed to two kinds of rhodium oxides with different extent of interaction with Al_2O_3 (i.e. RhO_x and Rh^iO_x). The peak with maximum above 1000 °C may have (at least partially) resulted from $Rh(AlO_2)_y$ species. With the decreasing of Rh loadings, O_2 desorption peaks shifted significantly to high temperature, indicating that the percentage of the rhodium species intimately interacting with the Al_2O_3 surface (Rh^iO_x) and that strongly interacting with the support ($Rh(AlO_2)_y$) increase significantly with the decreasing of Rh loadings. This is in good agreement with the results of TPR experiments.

The results of above H_2-TPR and O_2-TPD characterizations on the Rh/Al_2O_3 catalysts with different Rh loadings clearly indicate that, compared to the oxidized rhodium species in the catalysts with Rh loadings higher than 1 wt%, most of the oxidized rhodium species in the samples with Rh loadings $\leq$ 0.25 wt% possess stronger Rh–O bond and are more difficult to be reduced by H_2. These factors should be responsible for the significant difference in the catalytic performance of the catalysts for POM reaction.

3.3. High temperature in situ Raman characterization

To further elucidate the effect of metal-support interaction on the redox property of the rhodium species in the catalysts under reaction atmosphere and its relationship with the ignition temperature of the catalysts for POM reaction, a comparative study using high temperature *in situ* Raman spectroscopy on the Rh/SiO_2 and Rh/Al_2O_3 catalysts under $CH_4/O_2/Ar = 2/1/45$ atmosphere were carried out at temperature from 30 to 600 °C.

Fig. 5 shows the Raman spectra of the Rh/Al_2O_3 catalysts with Rh loadings of 0.1, 0.25, 1 and 3 wt% recorded at the temperature indicated in the figure during stepwise heating of the previously reduced samples under $CH_4/O_2/Ar = 2/1/45$ atmosphere from 30 to 600 °C. The Raman spectra of 4 wt% Rh/SiO_2 (Fig. 6) recorded under same experimental condition are also shown for comparison. It was found that, as soon as the H_2-reduced catalysts were switched to $CH_4/O_2/Ar$ mixture at the room temperature, the Raman bands with maxima at ~545 and ~540 cm^{-1} were observed (spectra not shown) on Rh/Al_2O_3 and 4 wt% Rh/SiO_2, respectively. According to the results of H_2-TPR experiments (Fig. 3), the bands at ~540 cm^{-1} can be assigned to the rhodium oxide species in Rh/SiO_2, and that at ~545 cm^{-1} can be assigned to the rhodium oxide species with different extent of interaction with Al_2O_3 (i.e. RhO_x and/or Rh^iO_x). This observation indicates that the metallic rhodium species (at least those on the surface of metallic rhodium particles) in both catalyst systems can be oxidized by O_2 in reactant even at room temperature. As the temperature of samples increased, the Raman band of the rhodium oxide species in 4 wt% Rh/SiO_2 was found to disappear at the temperature between 350 and 400 °C, while the temperatures at which RhO_x and/or Rh^iO_x species in Rh/Al_2O_3 vanished depend on the Rh loadings. It is also found that the temperatures at which the rhodium oxide species in the Rh/SiO_2 or Rh/Al_2O_3 vanishes are in good agreement with the temperatures when the POM reaction over the catalyst ignites (see the catalytic performance of the catalysts shown in

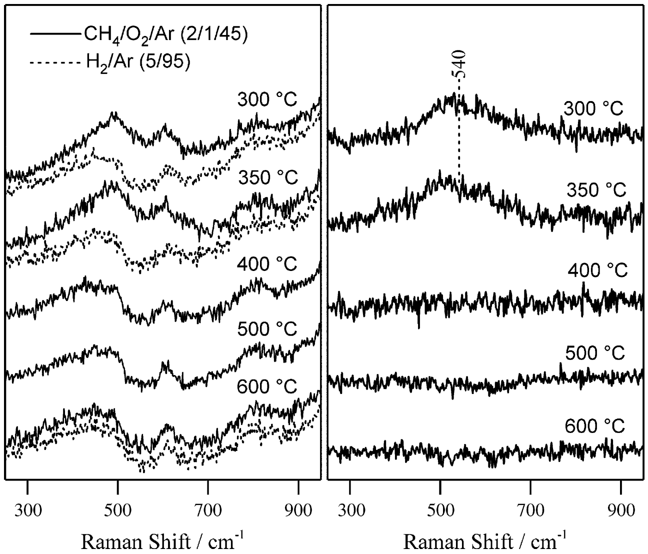

Fig. 6. Raman spectra of 4 wt% Rh/SiO$_2$ catalyst recorded at the indicated temperature during stepwise heating of the previously reduced samples under CH$_4$/O$_2$/Ar = 2/1/45 atmosphere (solid line) from 30 to 600 °C. The spectra recorded under H$_2$/Ar = 5/95 atmosphere (dotted line) are shown for comparison. Left: Original spectra. Right: The spectra of SiO$_2$ were subtracted.

Table 2). These results indicate that, the rhodium species in oxidized form are mainly responsible for complete oxidation of CH$_4$ to CO$_2$ and H$_2$O. An abruptly change in the oxidation state of rhodium species in the catalyst take place at the temperature when POM reaction starts. The results of above *in situ* Raman characterization have also provided further experimental evidence that the rhodium species in the Rh/Al$_2$O$_3$ catalysts with Rh lower loadings possess higher oxygen affinity and are more difficult to be reduced than those in the catalysts with higher Rh loadings under the POM reaction atmosphere.

On the basis of the results of H$_2$-TPR, O$_2$-TPD and *in situ* Raman characterizations shown above, the difference in the ignition temperatures of POM reaction over the Rh/Al$_2$O$_3$ catalysts with different Rh loadings can be related to the difference in the proportion of RhO$_x$ and Rh^{i}O$_x$ species in the catalyst samples. The results of catalytic performance test (Table 2) and *in situ* Raman characterization (Fig. 5) clearly indicated that POM reaction over Rh/Al$_2$O$_3$ started at the temperature when most of the rhodium oxides species (RhO$_x$ and Rh^{i}O$_x$) were reduced to metallic state. The ignition temperatures for the POM reaction over the catalyst are therefore closely related to the temperature at which most of the RhO$_x$ and Rh^{i}O$_x$ species can be reduced by CH$_4$ in the reaction mixture. Compared to the Rh/Al$_2$O$_3$ with high Rh loading, the catalyst with low Rh loading contains more Rh^{i}O$_x$ species which possess stronger Rh–O bond strength and are more difficult to be reduced than RhO$_x$ under the POM atmosphere. As a result, higher temperature is required to ignite the POM reaction over the catalysts with lower Rh loadings.

As can be seen from the results of H$_2$-TPR and O$_2$-TPD characterizations (Figs. 2 and 4, Table 3), A major difference between the Rh/Al$_2$O$_3$ catalysts of high (≥1 wt%) and low (≤0.25 wt%) Rh loadings is that the proportion of the rhodium species of different reducibility (i.e. RhO$_x$, Rh^{i}O$_x$ and Rh(AlO$_2$)$_y$) is significantly different. The catalysts with Rh loadings above 1 wt% contain more than 56% of rhodium oxide species (i.e. RhO$_x$ and Rh^{i}O$_x$) which can be easily reduced by H$_2$ at the temperature below 350 °C, while in the catalysts with Rh loadings below 0.25 wt%, the percentage of the rhodium species formed by diffusion of rhodium oxides into sublayers of Al$_2$O$_3$ structure (i.e, Rh(AlO$_2$)$_y$) increases significantly. Since steady-state activity for POM reaction were observed over the catalysts with Rh loadings higher than 1 wt%, the origin of the oscillatory behaviour during the reaction over the Rh/Al$_2$O$_3$ with Rh loadings below 0.25 wt% should be related to the formation of large percentage (≥70%) of Rh(AlO$_2$)$_y$ species which could only be reduced by H$_2$ at the temperature above 500 °C. Based on the results of mass spectrometry study on the reaction over 0.1 wt% Rh/Al$_2$O$_3$ catalyst at 600 and 850 °C, the oscillatory behaviour during POM reaction can be explained by cyclically switching of the Rh(AlO$_2$)$_y$ species from the oxidized state to the reduced state as a result of temperature oscillation in the catalyst bed during the reaction. While the temperature of the catalyst during the reaction is governed by the change in the proportion of the following exothermic and endothermic reactions, i.e. total oxidation of methane to CO$_2$ and H$_2$O (1), partial oxidation of methane (2), steam reforming of methane (3) and CO$_2$ reforming of methane (4) to synthesis gas.

$$CH_4 + 2O_2 \rightarrow CO_2 + 2H_2O \quad \Delta H^\circ_{(298K)} = -803\,\text{kJ/mol} \tag{1}$$

$$CH_4 + 1/2O_2 \rightarrow CO + 2H_2 \quad \Delta H^\circ_{(298K)} = -36\,\text{kJ/mol} \tag{2}$$

$$CH_4 + H_2O \rightarrow CO + 3H_2 \quad \Delta H^\circ_{(298K)} = 206\,\text{kJ/mol} \tag{3}$$

$$CH_4 + CO_2 \rightarrow 2CO + 2H_2 \quad \Delta H^\circ_{(298K)} = 247\,\text{kJ/mol} \tag{4}$$

The change in the proportion of each reaction would change the overall reaction heat as well as the temperature of the catalyst. The main features of the oscillation in mass spectrometry signals observed in Fig. 2 marked by the letters (a–c) can therefore be explained as follows.

At point (a), the catalyst showed lowest activity for synthesis gas formation (~40% CO, selectivity) and highest activity for CH$_4$ combustion (~60% CO$_2$, selectivity). Since the oxidized rhodium species is a poorer catalyst than the metallic Rh for synthesis gas formation, the catalyst at this point can be thought to consist of mainly oxidized Rh species. However, based on the results of H$_2$-TPR (Fig. 3) and *in situ* Raman characterizations (Fig. 5), most of the RhO$_x$ and Rh^{i}O$_x$ species should have been reduced under the experimental condition. The dominant oxidized rhodium species in the catalyst can only be the Rh(AlO$_2$)$_y$ species. This species is thought to be active for the total oxidation of CH$_4$. Accompanied by the increase in the proportion of highly exothermic CH$_4$ combustion reaction (reaction (1)) on the catalyst, large amount of heat was produced, leading to an increase in catalyst bed temperature. When the temperature of the catalyst is high enough, some of the rhodium species in Rh(AlO$_2$)$_y$ are reduced, resulting in a sudden increase in the activity of the catalyst for synthesis gas formation via the slightly exothermic reaction (2) and/or strong endothermic reactions (3 and 4), as observed between points (a and b). At the same time, the proportion of highly exothermic CH_4 combustion reaction (reaction (1)) over the catalyst falls rapidly to a minimum value. As a result, the temperature of the catalyst gradually decrease, and the metallic rhodium species formed by the reduction of $Rh(AlO_2)_y$ at high temperature are slowly reoxidized to $Rh(AlO_2)_y$. Accompanied by the reoxidation of the catalyst, the rate of reactions (2–4) decreased and the activity of the catalyst for highly exothermic reaction (1) increased again, as observed between point (b and c). A new oscillation cycle will begin when temperature of the catalyst is high enough for the reduction of $Rh(AlO_2)_y$. If the furnace temperature is sufficient high (e.g. ≥ 850 °C), the reoxidation of metallic Rh species to $Rh(AlO_2)_y$ is restrained. Most of the rhodium species in the catalyst under reaction condition will remain in the metallic state. Thus, the oscillatory behaviour is no longer observed when the temperature of furnace is above 850 °C.

4. Conclusions

On the basis of the results of H_2-TPR, O_2-TPD and *in situ* Raman characterizations, it can be concluded that the ignition temperature for the POM reaction over Rh/Al_2O_3 catalysts is related to the temperature at which most of the RhO_x and Rh^iO_x species in the sample is reduced by CH_4 in the reaction mixture. Compared to the Rh/Al_2O_3 with high Rh loadings, the catalysts with low Rh loadings contain more Rh^iO_x species which possess stronger Rh–O bond strength and are more difficult to be reduced than RhO_x under POM reaction atmosphere. Higher temperature is therefore required to ignite the POM reaction over the catalysts with lower Rh loadings. The oscillation during POM reaction over the Rh/Al_2O_3 with low Rh loadings ($\leq$0.25 wt%) can be related to the behaviour of the $Rh(AlO_2)_y$ species (formed by diffusion of rhodium oxide into sublayers of Al_2O_3 structure) in the catalyst switching cyclically from the oxidized state to the reduced state during the reaction.

Acknowledgements

This project is supported by the Ministry of Science and Technology of China (2005CB221401), the National Natural Science Foundation of China (20433030 and 20423002) and Key Scientific Project of Fujian Province, China" (2005HZ01-3).

References

[1] M. Prettre, Ch. Eichner, M. Perrin, Trans. Faraday Soc. 42 (1946) 335.
[2] A.T. Ashcroft, A.K. Cheetham, J.S. Foord, M.L.H. Green, C.P. Grey, A.J. Murrell, P.D.F. Vernon, Nature 344 (1990) 319.
[3] D.A. Hickman, L.D. Schmidt, J. Catal. 138 (1992) 267.
[4] D.A. Hickman, L.D. Schmidt, Science 259 (1993) 343.
[5] Y.H. Hu, E. Ruckenstein, Adv. Catal. 48 (2004) 297, and the references there in.
[6] D.A. Hickman, L.D. Schmidt, AIChE J. 39 (1993) 1164.
[7] D. Dissanayake, M.P. Rosynek, K.C.C. Kharas, J.H. Lunsford, J. Catal. 132 (1991) 117.
[8] F. van Looij, E.R. Stobbe, J.W. Geus, Catal. Lett. 50 (1998) 59.
[9] O.V. Buyevskaya, D. Wolf, M. Baerns, Catal. Lett. 29 (1994) 249.
[10] E.P.J. Mallens, J.H.B.J. Hoebink, G.B. Marin, J. Catal. 167 (1997) 43.
[11] H.K. Hofstad, J.H.B.J. Hoebink, A. Holmen, G.B. Marin, Catal. Today 40 (1998) 157.
[12] M. Fathi, F. Monnet, Y. Schuurman, A. Holmen, C. Mirodatos, J. Catal. 190 (2000) 439.
[13] D.Z. Wang, O. Dewaele, A.M. De Groote, G.F. Froment, J. Catal. 159 (1996) 418.
[14] J.C. Slaa, R.J. Berger, G.B. Marin, Catal. Lett. 43 (1997) 63.
[15] W.Z. Weng, Q.G. Yan, C.R. Luo, Y.Y. Liao, H.L. Wan, Catal. Lett. 74 (2001) 37.
[16] W.Z. Weng, Q.G. Yan, C.R. Luo, Y.Y. Liao, M.S. Chen, H.L. Wan, Stud. Surf. Sci. Catal. 136 (2001) 233.
[17] W.Z. Weng, M.S. Chen, H.L. Wan, Chem. Rec. 2 (2002) 102.
[18] Y. Boucouvalas, Z.L. Zhang, X.E. Verykios, Catal. Lett. 40 (1996) 189.
[19] Y. Boucouvalas, Z.L. Zhang, A.M. Efstathiou, X.E. Verykios, Stud. Surf. Sci. Catal. 101 (1996) 443.
[20] V.R. Choudhary, A.M. Rajput, B. Prabhakar, J. Catal. 139 (1993) 326.
[21] V.R. Choudhary, A.S. Mamman, S.D. Sansare, Angew. Chem. Int. Ed. Engl. 31 (1992) 1189.
[22] V.R. Choudhary, A.M. Rajput, B. Prabhakar, Catal. Lett. 15 (1992) 363.
[23] V.R. Choudhary, A.M. Rajput, V.H. Rane, J. Phys. Chem. 96 (1992) 8686.
[24] C. Elmasides, D.I. Kondarides, W. Grünert, X.E. Verykios, J. Phys. Chem. 103 (1999) 5227.
[25] C. Elmasides, D.I. Kondarides, S.G. Neophytides, X.E. Verykios, J. Catal. 198 (2001) 195.
[26] H.Y. Wang, E. Ruckenstein, J. Catal. 186 (1999) 181.
[27] E. Ruckenstein, H.Y. Wang, J. Catal. 187 (1999) 151.
[28] E. Ruckenstein, H.Y. Wang, J. Catal. 190 (2000) 32.
[29] K. Nakagawa, N. Ikenaga, T. Suzuki, T. Kobayashi, M. Haruta, Appl. Catal. A Gen. 169 (1998) 281.
[30] K. Nakagawa, N. Ikenaga, Y. Teng, T. Kobayashi, T. Suzuki, J. Catal. 186 (1999) 405.
[31] F. Monnet, Y. Schuurman, F. Cadete Santos Aires, J.C. Bertolini, C. Mirodatos, Catal. Today 64 (2001) 51.
[32] Z.J. Tian, O. Dewaele, G.B. Marin, Catal. Lett. 57 (1999) 9.
[33] E. Kikuchi, Y. Chen, Stud. Surf. Sci. Catal. 119 (1998) 441.
[34] H.Y. Wang, E. Ruckenstein, Catal. Lett. 59 (1999) 121.
[35] J.B. Claridge, M.L.H. Green, S.C. Tsang, A.P.E. York, A.T. Ashcroft, P.D. Battle, Catal. Lett. 22 (1993) 299.
[36] J.D. Grunwaldt, L. Basini, B.S. Clausen, J. Catal. 200 (2001) 321.
[37] H.Y. Wang, E. Ruckenstein, J. Phys. Chem. B 103 (1999) 11327.
[38] R.S. Zhou, R.L. Snyder, Acta Cryst. B47 (1991) 617.
[39] W.Z. Weng, X.Q. Pei, J.M. Li, C.R. Luo, Y. Liu, H.Q. Lin, C.J. Huang, H.L. Wan, Catal. Today 117 (2006) 53.
[40] D. Dissanayake, M.P. Rosynek, J.H. Lunsford, J. Phys. Chem. 97 (1993) 3644.
[41] C.P. Hwang, C.T. Yeh, Q.M. Zhu, Catal. Today 51 (1999) 93.
[42] H.C. Yao, S. Japar, M. Shelef, J. Catal. 50 (1977) 407.
[43] X.L. Zhang, D.O. Hayward, D.M.P. Mingos, Catal. Lett. 83 (2002) 149.
[44] X.L. Zhang, D.O. Hayward, D.M.P. Mingos, Catal. Lett. 86 (2003) 235.
[45] X.L. Zhang, C.S.M. Lee, D.M.P. Mingos, D.O. Hayward, Appl. Catal. A Gen. 248 (2003) 129.
[46] X.L. Zhang, C.S.M. Lee, D.M.P. Mingos, D.O. Hayward, Appl. Catal. A Gen. 240 (2003) 183.
[47] X.L. Zhang, C.S.M. Lee, D.O. Hayward, D.M.P. Mingos, Catal. Today 105 (2005) 283.
[48] V.Yu. Bychkov, Yu.P. Tyulenin, M.M. Slinko, V.N. Korchak, Appl. Catal. A Gen. 321 (2007) 180.
[49] L. Basini, A. Guarinoni, A. Aragno, J. Catal. 190 (2000) 284.
[50] Y. Liu, W.P. Fang, W.Z. Weng, H.L. Wan, J. Mol. Catal. A-Chem. 239 (2005) 193.